ACS NANO
Cite This: ACS Nano 2019, 13, 10272−10278
www.acsnano.org

ARTICLE

Ultrafast Catalyst-Free Graphene Growth on Glass Assisted by Local Fluorine Supply

Yadian Xie,[†,#] Ting Cheng,[†,§,#] Can Liu,[‡,#] Ke Chen,[†,∥] Yi Cheng,[†] Zhaolong Chen,[†] Lu Qiu,[§] Guang Cui,[†] Yue Yu,[†] Lingzhi Cui,[†] Mengtao Zhang,[†] Jin Zhang,[†,⊥] Feng Ding,*[,§] Kaihui Liu,*[,‡,⊥] and Zhongfan Liu*[,†,⊥]

[†]Center for Nanochemistry, Beijing National Laboratory for Molecular Sciences, College of Chemistry and Molecular Engineering, Academy for Advanced Interdisciplinary Studies, Peking University, Beijing 100871, China

[‡]State Key Laboratory for Mesoscopic Physics, Collaborative Innovation Center of Quantum Matter, School of Physics, Academy for Advanced Interdisciplinary Studies, Peking University, Beijing 100871, China

[§]Centre for Multidimensional Carbon Materials, Institute for Basic Science, School of Materials Science and Engineering, Ulsan National Institute of Science and Technology, Ulsan 44919, Korea

[⊥]Beijing Graphene Institute (BGI), Beijing 100095, China

[∥]Institute of Micro/Nano Photonic Materials and Applications, School of Physics and Electronics, Henan University, Kaifeng 475004, China

Supporting Information

ABSTRACT: **High-quality graphene film grown on dielectric substrates by a direct chemical vapor deposition (CVD) method promotes the application of high-performance graphene-based devices in large scale. However, due to the noncatalytic feature of insulating substrates, the production of graphene film on them always has a low growth rate and is time-consuming (typically hours to days), which restricts real potential applications. Here, by employing a local-fluorine-supply method, we have pushed the massive fabrication of a graphene film on a wafer-scale insulating substrate to a short time of just 5 min without involving any metal catalyst. The highly enhanced domain growth rate (~37 nm min^{-1}) and the quick nucleation rate (~1200 nuclei min^{-1} cm^{-2}) both account for this high productivity of graphene film. Further first-principles calculation demonstrates that the released fluorine from the fluoride substrate at high temperature can rapidly react with CH_4 to form a more active carbon feedstock, CH_3F, and the presence of CH_3F molecules in the gas phase much lowers the barrier of carbon attachment, providing sufficient carbon feedstock for graphene CVD growth. Our approach presents a potential route to accomplish exceptionally large-scale and high-quality graphene films on insulating substrates, *i.e.*, SiO_2, SiO_2/Si, fiber, *etc.*, at low cost for industry-level applications.**

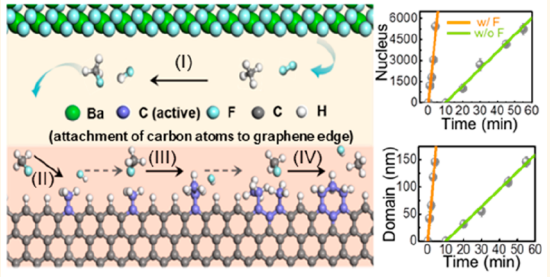

KEYWORDS: *graphene, ultrafast growth, catalyst-free, local fluorine supply, glass*

The excellent physical properties of graphene[1−3] have made it an attractive candidate for wide applications in electronic,[4,5] optoelectronic,[6−8] and photovoltaic devices.[9−12] But to fully realize and maximize the potential of graphene on integrated circuits, it should be compatible with the semiconducting or insulating wafer. Among various graphene synthesis strategies,[13−15] the chemical vapor deposition (CVD) method has notable advantages for the synthesis of high-quality and industrial-scale graphene products with flexible controllability.[16] However, for the conventional CVD-grown graphene on metal, a complex and cumbersome transfer process is inevitable for device fabrication on the target substrates (usually semiconductor or insulator). Meanwhile, the quality of graphene largely degrades due to the wrinkles, defects, and contaminants involved in this treatment, which in turn limits the performance in electronic devices.[17−19] Therefore, the way toward the direct growth of graphene on insulating substrates without involving any chemical catalyst is in great demand to make it be satisfactory for various device applications.

In previous studies, graphene has been successfully grown on different substrates, such as SiO_2,[20,21] Al_2O_3,[22] Si_3N_4,[23] and BN,[24,25] *via* a direct CVD method. Herein, the combination of graphene endows traditional glass with excellent hydro-

Received: May 9, 2019
Accepted: August 20, 2019
Published: August 20, 2019

Downloaded via PEKING UNIV on October 9, 2020 at 06:17:48 (UTC).
See https://pubs.acs.org/sharingguidelines for options on how to legitimately share published articles.

© 2019 American Chemical Society

DOI: 10.1021/acsnano.9b03596
ACS Nano 2019, 13, 10272−10278

phobicity, as well as high thermal and electrical conductivity, without sacrificing its original optical transparency.[26] However, due to the weak pyrolysis capability of carbon precursors and the lack of catalytic activity, a long growth time (typically hours to days) is required for graphene synthesis on dielectric substrates, limiting the mass production and industrial applications of graphene glass.[27−29] In principle, the production efficiency of graphene film largely relies on two important factors, *i.e.*, the nucleation rate and the growth rate of an individual domain. Recently, great efforts have been undertaken toward a higher growth rate of graphene on dielectric substrates by predeposition or evaporation of catalytic metals, such as copper or nickel, to enhance the thermal decomposition efficiency of hydrocarbon.[30−33] However, it is usually a time-consuming and high-cost process with metal residues decreasing the quality of graphene film. Other attempts, such as using special precursors (cyclohexane, acetylene, ethanol, *etc.*) with low pyrolysis energy barriers, have been employed to improve the growth rate of graphene on insulating substrates as well, but quality and layer numbers cannot be controlled well.[34−38] Finding a low-cost catalyst-free graphene growth method without sacrificing the material's quality becomes extremely essential to overcome the bottleneck in graphene-based electronics.

In this article, we design a local-fluorine-supply method to realize the ultrafast growth of graphene on a quartz glass wafer with well-controlled uniformity. Fluorine is introduced by the decomposition of metal fluoride at high temperature and confined in the narrow gap between the quartz glass and fluoride surfaces. During the growth process, the localized high concentration of fluorine will substitute hydrogen in methane and form a more active carbon feedstock, *i.e.*, CH_3F. The presence of CH_3F molecules in the gas phase greatly lowers the barrier of carbon addition, providing sufficient carbon feedstock for graphene CVD growth. Meanwhile, intermolecular collisions between active carbon species are significantly enhanced in the confined space between quartz glass and fluoride. All these changes caused by the local-fluorine-supply design benefit the massive production of graphene film on a quartz wafer: the graphene growth rate is enhanced to ∼37 nm min^{-1}, while the nucleation rate increases to ∼1200 nuclei min^{-1} cm^{-2}. We finally push the massive production of graphene film on a wafer-scale insulating substrate to a short time of just 5 min without involving any metal catalyst, which promotes the low-cost, high-productivity graphene film compatible with a semiconductor circuit.

RESULTS AND DISCUSSION

In our experiment on graphene growth, quartz glass was directly placed above a metal fluoride substrate with a naturally formed ∼30 μm gap between them (Figure 1a and Figure S1). To prove that the fluorine can emit from the fluoride substrate to the confined space of the gap, we annealed a 10 nm BaF_2/Si substrate (BaF_2 film was deposited by electron beam evaporation) with a quartz placed above it under graphene growth conditions. Then, X-ray photoelectron spectroscopy (XPS) was employed to measure the signal of fluorine. The result showed that the peak of fluorine disappeared after annealing at high temperature and proved that the fluorine can emit from the surface of the metal fluoride (Figure 1b). To study the role of the local fluorine in graphene growth, we designed a comparison experiment to show the differences in growth behavior between the fluorine-supply growth and

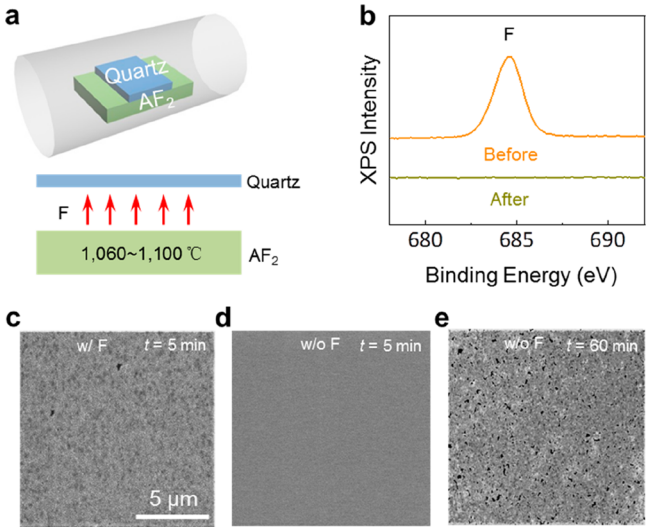

Figure 1. Catalyst-free growth of graphene on glass assisted by local fluorine supply. (a) Diagram of the experimental design and the lateral view of the gap between metal fluoride AF_2 and quartz surface. (b) XPS of the BaF_2/Si substrate (BaF_2 thickness ∼10 nm) annealing at ∼1000 °C in a CVD system. The absence of the fluorine peak is indicative of the evaporation of fluorine from the BaF_2 at high temperatures. (c, d) Comparison of the SEM images of graphene on the surfaces of the ST-cut quartz after 5 min growth supported by BaF_2 (c) and quartz glass (d). (e) SEM images of graphene on the surface of the ST-cut quartz at 60 min using quartz glass as the supporting substrate.

common non-fluorine-involved growth. Scanning electron microscopy (SEM) was conducted to analyze the growth results of as-synthesized graphene on quartz glass substrates. Graphene film with full coverage was grown on the surface of ST-cut quartz glass that faces the BaF_2 substrate within 5 min (Figure 1c). In contrast, graphene domains did not appear on the surface of ST-cut quartz glass that was laid on the commonly used quartz substrate within 5 min (Figure 1d), and it reached nearly full coverage at around 60 min (Figure 1e), which showed a typical growth behavior like that in sapphire or SiO_2/Si (Figure S2a,b). Other different fluoride substrates, CaF_2 and MgF_2 (Figure S2c,d), were also examined, and both of them had comparable effects on the graphene growth to that of BaF_2. In addition, the introduction of fluorine showed the same effect on the growth of graphene on SiO_2/Si as well (Figure S3a,b). Based on the above phenomena, a significant signature is found: fluorine can emit from the fluoride substrate and is confined in the narrow space, which exerted a critical effect in facilitating the ultrafast graphene growth on various substrates.

The quality of graphene films on a quartz glass substrate by the local-fluorine-supply method was confirmed by high-resolution transmission electron microscopy (HRTEM), which demonstrated that most of the samples are primarily monolayers with limited few-layer regions (Figure 2a,b, Figure S4, and Figure S5). Moreover, an abberation-corrected TEM image (Figure 2c) indicated the high crystallinity of the as-grown graphene. The fast Fourier transform (FFT) pattern further confirmed the perfect single-layer characteristics. The diminished 2D/G peak intensity in the Raman spectrum illustrated that the thickness of the graphene film increased with the growth time (Figure 2d), and the Raman mapping of transferred graphene demonstrated the high uniformity of the

DOI: 10.1021/acsnano.9b03596
ACS Nano 2019, 13, 10272−10278

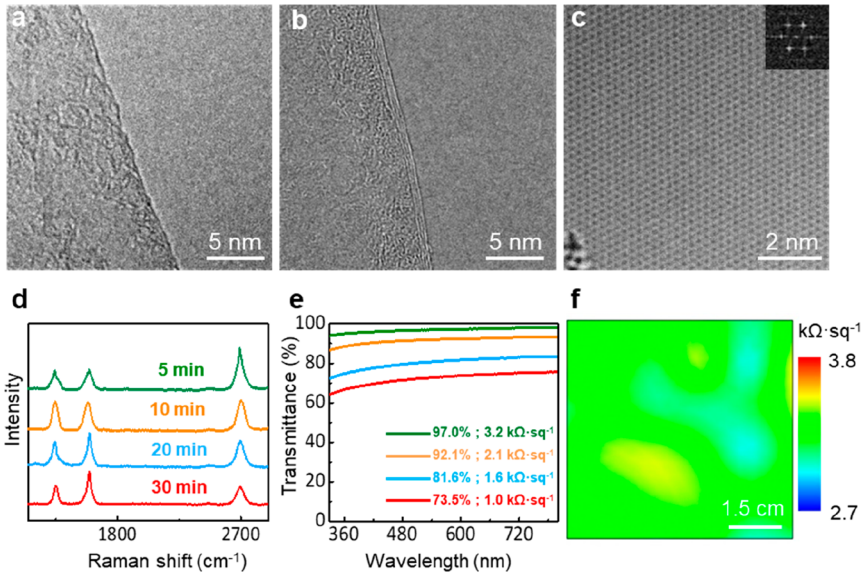

Figure 2. Quality characterization of the graphene film by the local-fluorine-supply method. (a, b) HRTEM images of monolayer (a) and multilayer (b) graphene regions grown in 5 min. (c) Atomic-resolution TEM image of monolayer graphene. The inset is the corresponding fast Fourier transform pattern. (d) Raman spectra of graphene film on quartz glass after different growth times. (e) Correlation of UV−vis transmittance and sheet resistance of the graphene/quartz glass after different growth times. (f) Mapping of the sheet resistance on a 5 × 5 cm^2 area of graphene film on an ST-cut quartz glass plate.

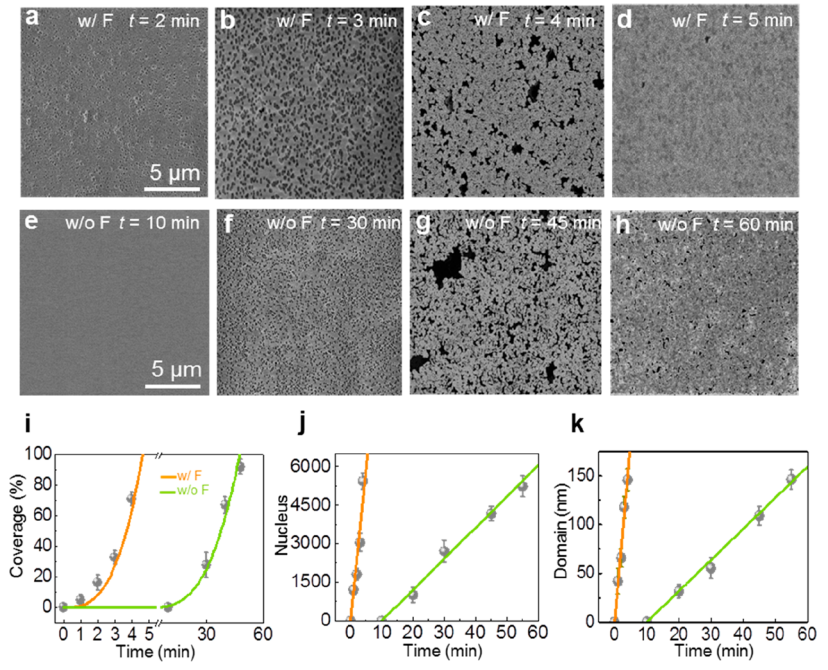

Figure 3. Comparison of graphene film between BaF_2 confined growth and quartz glass confined growth. (a−d) SEM images of graphene growth assisted by fluorine at t = 2, 3, 4, and 5 min, respectively. (e−h) SEM images of graphene growth assisted by quartz confined flow at t = 10, 30, 45, and 60 min. (i) Coverage of graphene as a function of growth time using BaF_2 and quartz as supporting substrates. (j) Number of nuclei of graphene as a function of growth time using BaF_2 and quartz glass as supporting substrates. It indicates an ultrafast nuclei rate of ∼1200 min^{-1} cm^{-2} with BaF_2 assistance, which is much larger than that of the quartz confined flow method (∼130 min^{-1} cm^{-2}). (k) Time evolution of the domain size by using BaF_2 and quartz as supporting substrate. The growth rate of graphene assisted by fluorine (∼37 nm min^{-1}) is much larger than that of quartz confined flow (∼3 nm min^{-1}). The error bars represent the standard error from the measurement of 20 samples.

as-grown graphene film (Figure S6) with comparable quality with that of graphene without fluorine assistance (Figure S7).

Moreover, the transparency and sheet resistance were characterized by UV−vis transmittance spectroscopy and the four-probe method to test the capacity of optical and electrical modulation. The monolayer graphene film, which was obtained within just 5 min, showed a 97.0% transmittance at a wavelength of 550 nm, along with an average sheet resistance of ∼3.2 kΩ·sq^{-1} (Figure 2e). The mapping of sheet resistance on the wafer-scale film (5 × 5 cm^2) reveals the uniform

DOI: 10.1021/acsnano.9b03596
ACS Nano 2019, 13, 10272−10278

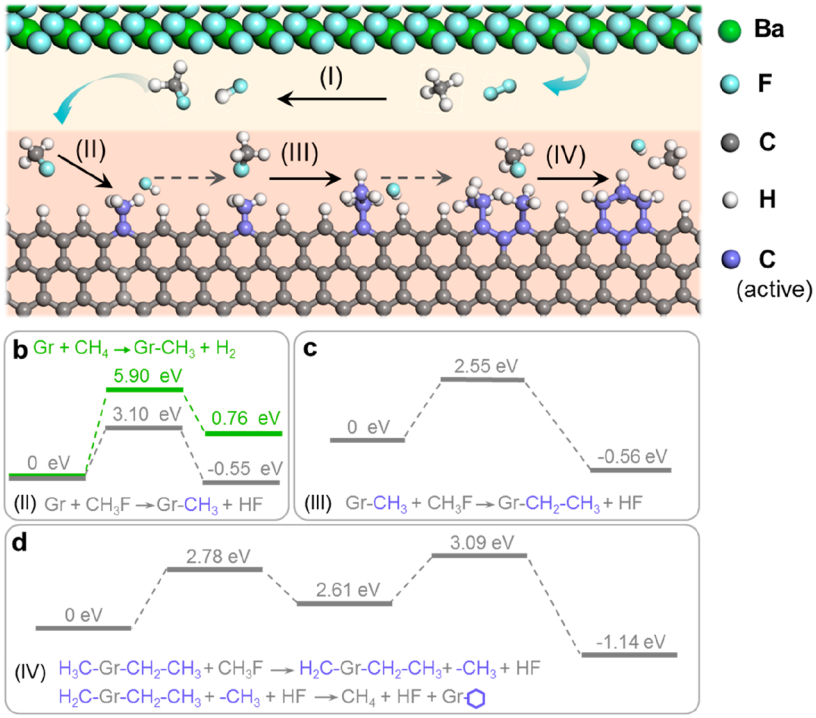

Figure 4. Mechanism for the local-fluorine-assisted growth of graphene. (a) Schematic diagrams of a possible reaction route for graphene growth with the assistance of metal fluoride, where the formation of CH_3F (I) in the gas phase is a key step that greatly lowers the barrier of carbon attachment to the edge of graphene (II, III, and IV). The energy profile for reaction I is shown in Figure S10 in the Supporting Information. (b) The energy profile for reaction II: the reaction of a CH_3F molecule with a graphene zigzag edge (gray). For comparison, the energy profile for the reaction of a CH_4 molecule (green) is also presented. (c) The energy profile for reaction III: the attachment of the second carbon by decomposing another CH_3F molecule at the edge. (d) The energy profile for step IV: three added carbons form a new hexagonal ring at the graphene zigzag edge with the assistance of another CH_3F molecule. To clearly show the process, the carbon atoms of the new hexagon are marked by purple. In the above reactions, the CH_3F molecules play two critical roles: (i) as an easily decomposed carbon source to lower the barrier of carbon attachment and (ii) to remove the additional H atoms from the edge of graphene.

resistance of the as-grown graphene on quartz glass (Figure 2f). In addition, the sheet resistance decreases by further lengthening the growth time of graphene, which demonstrates to be efficient in tuning the performance of the transparent conducing electrode (TCE). Furthermore, the C 1s XPS spectrum showed the featured signals of graphene, which included an sp^2 carbon peak (284.8 eV), a C−H peak (285.5 eV), and a broad C−O peak.[39] The absence of a F 1s peak and C−F bonds of the as-grown graphene film (Figure S8) indicates the high quality of graphene on glass without fluorine doping.

In order to study the ultrafast growth behavior of graphene domains on a quartz glass substrate, two different synthesis methods were compared in detail: (i) the local-fluorine-supply method and (ii) the commonly used confined-flow method supported by a quartz substrate. After a growth time of *t*, the system heating and carbon source supply were stopped instantly, and a large flux of Ar gas was flushed in. The SEM images (Figure 3a−d) illustrated that, with the support of a fluoride substrate, a large amount of graphene nuclei occurred within 2 min, and the graphene domains grew rapidly, achieving full coverage on ST-cut quartz glass in only 5 min. The domain growth rate was ∼37 nm min^{-1}, and the nucleation rate reached ∼1200 nuclei min^{-1} cm^{-2} (Figure 3i−k). In contrast, the growth rate was much lower with the support of a quartz substrate (Figure 3e−h): no domain was observed on the ST-cut quartz glass even after the feedstock supply by 10 min. The nucleation started at around 20 min, and full coverage occurred after at least 60 min. The domain growth rate was ∼3 nm min^{-1}, and the domain nucleation rate was ∼130 nuclei min^{-1} cm^{-2} (Figure 3i−k). The results of mass spectroscopy (Figure S9) indicated that utilization efficiency of CH_4 with fluorine assistance is about 15% higher than that without fluorine. Notably, it is of particular interest that the domain growth rates and nucleation rates were enhanced by approximately 12 and 9 times, respectively, in the fluorine-local-supply approach. These results demonstrate that the active carbon feedstock is greatly enhanced in our designed growth system. Such a growth rate is much faster than other reported rates (Table S1, Supporting Information, comparing to previous values on quartz substrate).

To further evaluate the graphene coverage with time, a nonlinear fitting was used (Figure 3i). The coverage is equal to the total of the whole graphene domain areas on the surface, as well as proportional to the cube of growth time. Therefore, a mathematic expression of the total coverage is given as

$$A = \sum Ai \sim 1.15t^3 \quad (1)$$

where *t* starts at $t = 0$ when the growth of the graphene domain occurs on the surface of ST-cut quartz glass. Based on our experimental analysis and the fitting value, homogeneous graphene film on glasses with 100% coverage can be rapidly fabricated in ∼4−5 min, which may benefit the mass production of low-cost, high-speed, and performance-tunable TCE.

DOI: 10.1021/acsnano.9b03596
ACS Nano 2019, 13, 10272−10278

The ultrafast growth of graphene on a quartz glass supported by a local fluorine supply has been demonstrated in our experiment. To understand the role of the local fluorine on graphene growth, we performed density functional theory (DFT) calculations to reveal a comprehensive picture of graphene growth at the atomic level. Considering the fact that the growth is in the environment with abundant H_2 gas and the quartz glass must be catalytically inert, a graphene nanoribbon (GNR) with hydrogen-terminated zigzag edges was constructed to represent the growth front of a growing graphene island. As we are focusing on the role of fluorine in graphene growth that is confined in the gas phase, the role of the substrate in carbon feedstock decomposition and carbon attachment were not considered in this study.

As confirmed by the XPS measurement, the BaF_2 substrate will release fluorine to the narrow gap between BaF_2 and the quartz substrate at the growth temperature (as shown in Figure 4a). Since fluorine possesses a strong electronegativity, it can easily substitute the H in a CH_4 molecule to form CH_3F (see route I in Figure S10). The reaction barrier is only 0.66 eV, and the reaction is highly exothermic; therefore, we can expect that a considerable amount of CH_4 molecules was converted into CH_3F molecules in the narrow gap. The attachment of carbon atoms to the graphene edge by the collision of gas phase molecules with the graphene edge is a necessary step for the graphene growth. The calculated reaction barrier of a CH_4 molecule reacting with a graphene zigzag edge is as high as 5.90 eV, and the reaction is endothermic (green profile shown in Figure 4b and the concrete reaction process of the first step for CH_4 is shown in Figure S11). So, we can conclude that the direct reaction of CH_4 at a graphene edge is prohibited at the temperature of graphene growth (1300 K), which must result in a very slow growth rate of the graphene on a catalyst-free substrate. In sharp contrast, the reaction barrier of a CH_3F molecule with a graphene zigzag edge is just 3.10 eV, and the reaction is exothermic (gray profile shown in Figure 4b).

The low reaction barrier of carbon attachment to the graphene edge explains the role of fluorine in ultrafast catalyst-free graphene CVD growth. To further understand more details of the graphene growth with the appearance of a CH_3F molecule, we considered a route of adding two more carbon atoms and forming a new hexagonal carbon ring on the graphene zigzag edge (routes III and IV in Figure 4a and the reaction energy profile shown in Figure 4c,d). The barrier of the second carbon addition is 2.55 eV, and the third carbon addition is a repeatable step of the first carbon addition. The threshold barrier of forming a new hexagonal carbon ring is 3.09 eV (the concrete intermediate reaction process is shown in Figure S12), and all the reactions are exothermic. The above calculations showed two important roles of CH_3F in fast graphene CVD growth: first, as a more active carbon feedstock, the presence of CH_3F molecules in the gas phase lowers the barrier of carbon addition during graphene CVD growth; second, a CH_3F molecule can remove two terminating H atoms from two nearby carbon atoms of a growing graphene edge. Such a reaction creates two dangling bonds in the two nearby carbon atoms, which allows a new C−C bond to be formed between the nearby atoms. The two important roles ensure the ultrafast growth of graphene.

CONCLUSIONS

In conclusion, we have demonstrated a continuous local-fluorine-supply method to realize ultrafast graphene growth on a wafer-scale insulating substrate in just 5 min. The highly increased growth rate of graphene domains (~37 nm min^{-1}) and the quick nucleation rate (~1200 nuclei min^{-1} cm^{-2}) both account for this high productivity of graphene film. Further studies show that the released fluorine can rapidly react with CH_4 to form a more active carbon feedstock, CH_3F, in the gas phase, which greatly lowers the barrier of carbon attachment and provides sufficient carbon feedstock for graphene growth on a dielectric substrate. The ultrafast growth of graphene film on glass is much more propitious to the commercial-scale applications of optoelectronic devices, such as smart windows, touch panels, LED illumination, and liquid crystal screens, which spotlights its characteristic of transparent conducting. Our work blazes an effective path for attaining high-quality graphene films on wafer-scale insulating substrates in a quite short production time, which boosts the low-cost and massive manufacture of graphene-based substrates and diversifies further applications in electronics, optoelectronics, and photovoltaics devices.

METHODS

Growth of Graphene. Cleaned ST-cut quartz wafers were placed on a flat fluoride substrate, and then together they were loaded into a 3 in. quartz tube inside a three-temperature-zone furnace (Lindberg/Blue). The tube was flushed with 1000 sccm Ar to remove air for 5 min, and then the temperature was ramped to the growth temperature (1060−1100 °C) with 300 sccm Ar and 300 sccm H_2. Afterward, the H_2 was converted to 150 sccm with 20−37 sccm CH_4 introduced into the tube for graphene growth. Finally, the CVD system was promptly cooled to room temperature with 1000 sccm Ar.

Transfer of Graphene. Typically, the graphene samples were transferred by employing a wet etching method (using poly(methyl methacrylate) as mediated protector and 1:1 hydrofluoric acid/ethanol solution as etching solution).

Characterization. The SEM images were taken by a SEM (Hitachi S-4800) operating at 1 kV. Raman spectra were taken by a LabRAM HR-800 (Horiba) using 514 nm laser excitation. Transmittance was measured by UV−vis spectroscopy (PerkinElmer Lambda 950 spectrophotometer). The sheet resistance was tested by a four-probe resistance measuring meter (Guangzhou 4-probe Tech Co. Ltd., RTS-4). The quality of graphene films was further characterized by XPS (Kratos Analytical Axis-supra), TEM (FET Tecnai F20, operating at 200 kV), and AFM (Vecco Nanoscope IIIa). The atomically resolved images of graphene were obtained on a FEI Titan3 300-80 TEM operated at 80 kV.

ASSOCIATED CONTENT

Supporting Information

The Supporting Information is available free of charge on the ACS Publications website at DOI: 10.1021/acsnano.9b03596.

Additional information (PDF)

AUTHOR INFORMATION

Corresponding Authors

*E-mail: f.ding@unist.ac.kr.
*E-mail: khliu@pku.edu.cn.
*E-mail: zfliu@pku.edu.cn.

ORCID

Jin Zhang: 0000-0003-3731-8859
Feng Ding: 0000-0001-9153-9279
Kaihui Liu: 0000-0002-8781-2495
Zhongfan Liu: 0000-0003-0065-7988

Author Contributions

#Y.X., T.C., and C.L. contributed equally to this work.

DOI: 10.1021/acsnano.9b03596
ACS Nano 2019, 13, 10272−10278

Notes

The authors declare no competing financial interest.

ACKNOWLEDGMENTS

This work was supported by National Key R&D Program of China (2016YFA0200103 and 2016YFA0300903), Beijing Graphene Innovation Program (Z181100004818003), and the Institute for Basic Science (IBS-R019-D1), South Korea. The authors also acknowledge the usage of the IBS-CMCM high-performance computing system simulator.

REFERENCES

(1) Lee, C.; Wei, X.; Kysar, J. W.; Hone, J. Measurement of the Elastic Properties and Intrinsic Strength of Monolayer Graphene. *Science* **2008**, *321*, 385−388.

(2) Novoselov, K. S.; Geim, A. K.; Morozov, S. V.; Jiang, D.; Katsnelson, M. I.; Grigorieva, I. V.; Dubonos, S. V.; Firsov, A. A. Two-Dimensional Gas of Massless Dirac Fermions in Graphene. *Nature* **2005**, *438*, 197−200.

(3) Novoselov, K. S.; Geim, A. K.; Morozov, S. V.; Jiang, D.; Zhang, Y.; Dubonos, S. V.; Grigorieva, I. V.; Firsov, A. A. Electric Field Effect in Atomically Thin Carbon Films. *Science* **2004**, *306*, 666−669.

(4) Balandin, A. A. Thermal Properties of Graphene and Nanostructured Carbon Materials. *Nat. Mater.* **2011**, *10*, 569−581.

(5) Nair, R. R.; Blake, P.; Grigorenko, A. N.; Novoselov, K. S.; Booth, T. J.; Stauber, T.; Peres, N. M. R.; Geim, A. K. Fine Structure Constant Defines Visual Transparency of Graphene. *Science* **2008**, *320*, 1308−1308a.

(6) Han, T. H.; Lee, Y.; Choi, M. R.; Woo, S. H.; Bae, S. H.; Hong, B. H.; Ahn, J. H.; Lee, T. W. Extremely Efficient Flexible Organic Light-Emitting Diodes with Modified Graphene Anode. *Nat. Photonics* **2012**, *6*, 105−110.

(7) Meric, I.; Han, M. Y.; Young, A. F.; Ozyilmaz, B.; Kim, P.; Shepard, K. L. Current Saturation in Zero-Bandgap, Top-Gated Graphene Field-Effect Transistors. *Nat. Nanotechnol.* **2008**, *3*, 654−659.

(8) Suk, J. W.; Lee, W. H.; Lee, J.; Chou, H.; Piner, R. D.; Hao, Y.; Akinwande, D.; Ruoff, R. S. Enhancement of the Electrical Properties of Graphene Grown by Chemical Vapor Deposition *via* Controlling the Effects of Polymer Residue. *Nano Lett.* **2013**, *13*, 1462−1467.

(9) Xia, F.; Mueller, T.; Lin, Y.-m.; Valdes-Garcia, A.; Avouris, P. Ultrafast Graphene Photodetector. *Nat. Nanotechnol.* **2009**, *4*, 839−843.

(10) Gabor, N. M.; Song, J. C. W.; Qiong, M.; Nair, N. L.; Thiti, T.; Kenji, W.; Takashi, T.; Levitov, L. S.; Pablo, J. H. Hot Carrier-Assisted Intrinsic Photoresponse in Graphene. *Science* **2011**, *334*, 648−52.

(11) Han, T. H.; Kwon, S. J.; Li, N.; Seo, H. K.; Xu, W.; Kim, K. S.; Lee, T. W. Versatile p-Type Chemical Doping to Achieve Ideal Flexible Graphene Electrodes. *Angew. Chem., Int. Ed.* **2016**, *55*, 6197−6201.

(12) Han, T. H.; Park, M. H.; Kwon, S. J.; Bae, S. H.; Seo, H. K.; Cho, H.; Ahn, J. H.; Lee, T. W. Approaching Ultimate Flexible Organic Light-Emitting Diodes Using a Graphene Anode. *NPG Asia Mater.* **2016**, *8*, No. e303.

(13) Novoselov, K. S.; Fal'Ko, V. I.; Colombo, L.; Gellert, P. R.; Schwab, M. G.; Kim, K. A Roadmap for Graphene. *Nature* **2012**, *490*, 192−200.

(14) Paton, K. R.; Eswaraiah, V.; Claudia, B.; Smith, R. J.; Umar, K.; Arlene, O. N.; Conor, B.; Mustafa, L.; Istrate, O. M.; Paul, K. Scalable Production of Large Quantities of Defect-Free Few-Layer Graphene by Shear Exfoliation in Liquids. *Nat. Mater.* **2014**, *13*, 624−630.

(15) Ohta, T.; Bostwick, A.; Seyller, T.; Horn, K.; Rotenberg, E. Controlling the Electronic Structure of Bilayer Graphene. *Science* **2006**, *313*, 951−954.

(16) Li, X.; Cai, W.; An, J.; Kim, S.; Nah, J.; Yang, D.; Piner, R.; Velamakanni, A.; Jung, I.; Tutuc, E.; Banerjee, S. K.; Colombo, L.; Ruoff, R. S. Large-Area Synthesis of High-Quality and Uniform Graphene Films on Copper Foils. *Science* **2009**, *324*, 1312−1314.

(17) Gao, L.; Ni, G.-X.; Liu, Y.; Liu, B.; Castro Neto, A. H.; Loh, K. P. Face-to-Face Transfer of Wafer-Scale Graphene Films. *Nature* **2014**, *505*, 190−194.

(18) Bae, S.; Kim, H.; Lee, Y.; Xu, X.; Park, J.-S.; Zheng, Y.; Balakrishnan, J.; Lei, T.; Ri Kim, H.; Song, Y. I.; Kim, Y.-J.; Kim, K. S.; Ozyilmaz, B.; Ahn, J.-H.; Hong, B. H.; Iijima, S. Roll-to-Roll Production of 30-Inch Graphene Films for Transparent Electrodes. *Nat. Nanotechnol.* **2010**, *5*, 574−578.

(19) Liang, X.; Sperling, B. A.; Calizo, I.; Cheng, G.; Hacker, C. A.; Zhang, Q.; Obeng, Y.; Yan, K.; Peng, H.; Li, Q.; Zhu, X.; Yuan, H.; Hight Walker, A. R.; Liu, Z.; Peng, L.-m.; Richter, C. A. Toward Clean and Crackless Transfer of Graphene. *ACS Nano* **2011**, *5*, 9144−9153.

(20) Chen, J.; Wen, Y.; Guo, Y.; Wu, B.; Huang, L.; Xue, Y.; Geng, D.; Wang, D.; Yu, G.; Liu, Y. Oxygen-Aided Synthesis of Polycrystalline Graphene on Silicon Dioxide Substrates. *J. Am. Chem. Soc.* **2011**, *133*, 17548−17551.

(21) Chen, J.; Guo, Y.; Jiang, L.; Xu, Z.; Huang, L.; Xue, Y.; Geng, D.; Wu, B.; Hu, W.; Yu, G.; Liu, Y. Near-Equilibrium Chemical Vapor Deposition of High-Quality Single-Crystal Graphene Directly on Various Dielectric Substrates. *Adv. Mater.* **2014**, *26*, 1348−1353.

(22) Wei, D.; Lu, Y.; Han, C.; Niu, T.; Chen, W.; Wee, A. T. S. Critical Crystal Growth of Graphene on Dielectric Substrates at Low Temperature for Electronic Devices. *Angew. Chem., Int. Ed.* **2013**, *52*, 14121−14126.

(23) Chen, J.; Guo, Y.; Wen, Y.; Huang, L.; Xue, Y.; Geng, D.; Wu, B.; Luo, B.; Yu, G.; Liu, Y. Two-Stage Metal-Catalyst-Free Growth of High-Quality Polycrystalline Graphene Films on Silicon Nitride Substrates. *Adv. Mater.* **2013**, *25*, 992−997.

(24) Gao, T.; Song, X.; Du, H.; Nie, Y.; Chen, Y.; Ji, Q.; Sun, J.; Yang, Y.; Zhang, Y.; Liu, Z. Temperature-Triggered Chemical Switching Growth of In-Plane and Vertically Stacked Graphene-Boron Nitride Heterostructures. *Nat. Commun.* **2015**, *6*, 6835.

(25) Wang, L.; Wu, B.; Chen, J.; Liu, H.; Hu, P.; Liu, Y. Monolayer Hexagonal Boron Nitride Films with Large Domain Size and Clean Interface for Enhancing the Mobility of Graphene-Based Field-Effect Transistors. *Adv. Mater.* **2014**, *26*, 1559−1564.

(26) Sun, J.; Chen, Z.; Yuan, L.; Chen, Y.; Ning, J.; Liu, S.; Ma, D.; Song, X.; Priydarshi, M. K.; Bachmatiuk, A. Direct Chemical-Vapor-Deposition-Fabricated, Large-Scale Graphene Glass with High Carrier Mobility and Uniformity for Touch Panel Applications. *ACS Nano* **2016**, *10*, 11136−11144.

(27) Chen, Y.; Sun, J.; Gao, J.; Du, F.; Han, Q.; Nie, Y.; Chen, Z.; Bachmatiuk, A.; Priydarshi, M. K.; Ma, D. Growing Uniform Graphene Disks and Films on Molten Glass for Heating Devices and Cell Culture. *Adv. Mater.* **2015**, *27*, 7839−7846.

(28) Sun, J.; Chen, Y.; Priydarshi, M. K.; Chen, Z.; Bachmatiuk, A.; Zou, Z.; Chen, Z.; Song, X.; Gao, Y.; Rummeli, M. H.; Zhang, Y.; Liu, Z. Direct Chemical Vapor Deposition-Derived Graphene Glasses Targeting Wide Ranged Applications. *Nano Lett.* **2015**, *15*, 5846−5854.

(29) Sun, J.; Chen, Y.; Priydarshi, M. K.; Gao, T.; Song, X.; Zhang, Y.; Liu, Z. Graphene Glass from Direct CVD Routes: Production and Applications. *Adv. Mater.* **2016**, *28*, 10333−10339.

(30) Kwak, J.; Chu, J. H.; Choi, J. K.; Park, S. D.; Go, H.; Kim, S. Y.; Park, K.; Kim, S. D.; Kim, Y. W.; Yoon, E. Near Room-Temperature Synthesis of Transfer-Free Graphene Films. *Nat. Commun.* **2012**, *3*, 645.

(31) Teng, P.-Y.; Lu, C.-C.; Akiyama-Hasegawa, K.; Lin, Y.-C.; Yeh, C.-H.; Suenaga, K.; Chiu, P.-W. Remote Catalyzation for Direct Formation of Graphene Layers on Oxides. *Nano Lett.* **2012**, *12*, 1379−1384.

(32) Su, C. Y.; Lu, A. Y.; Wu, C. Y.; Li, Y. T.; Liu, K. K.; Zhang, W.; Lin, S. Y.; Juang, Z. Y.; Zhong, Y. L.; Chen, F. R. Direct Formation of Wafer Scale Graphene Thin Layers on Insulating Substrates by Chemical Vapor Deposition. *Nano Lett.* **2011**, *11*, 3612−3616.

(33) Vang, R. T.; Honkala, K.; Dahl, S.; Vestergaard, E. K.; Schnadt, J.; Lægsgaard, E.; Clausen, B. S.; Nørskov, J. K.; Besenbacher, F.

DOI: 10.1021/acsnano.9b03596
ACS Nano 2019, 13, 10272−10278

Controlling the Catalytic Bond-Breaking Selectivity of Ni Surfaces by Step Blocking. *Nat. Mater.* **2005**, *4*, 160−162.
(34) Kim, K. B.; Lee, C. M.; Choi, J. Catalyst-Free Direct Growth of Triangular Nano-Graphene on All Substrates. *J. Phys. Chem. C* **2011**, *115*, 14488−14493.
(35) Miyasaka, Y.; Nakamura, A.; Temmyo, J. Graphite Thin Films Consisting of Nanograins of Multilayer Graphene on Sapphire Substrates Directly Grown by Alcohol Chemical Vapor Deposition. *Jpn. J. Appl. Phys.* **2011**, *50*, 584−587.
(36) Rummeli, M. H.; Bachmatiuk, A.; Scott, A.; Borrnert, F.; Warner, J. H.; Hoffman, V.; Lin, J.-H.; Cuniberti, G.; Buchner, B. Direct Low-Temperature Nanographene CVD Synthesis over a Dielectric Insulator. *ACS Nano* **2010**, *4*, 4206−4210.
(37) Wang, H.; Yu, G. Direct CVD Graphene Growth on Semiconductors and Dielectrics for Transfer-Free Device Fabrication. *Adv. Mater.* **2016**, *47*, 4956−4975.
(38) Xue, Y.; Wu, B.; Jiang, L.; Guo, Y.; Huang, L.; Chen, J.; Tan, J.; Geng, D.; Luo, B.; Hu, W. Low Temperature Growth of Highly Nitrogen-Doped Single Crystal Graphene Arrays by Chemical Vapor Deposition. *J. Am. Chem. Soc.* **2012**, *134*, 11060−11063.
(39) Chen, Z.; Qi, Y.; Chen, X.; Zhang, Y.; Liu, Z. Direct CVD Growth of Graphene on Traditional Glass: Methods and Mechanisms. *Adv. Mater.* **2019**, *31*, 1803639.

DOI: 10.1021/acsnano.9b03596
ACS Nano 2019, 13, 10272−10278